IVYSPRING INTERNATIONAL PUBLISHER

Theranostics

2017; 7(13): 3326-3337. doi: 10.7150/thno.17089

Research Paper

In Vivo Cancer Cells Elimination Guided by Aptamer-Functionalized Gold-Coated Magnetic Nanoparticles and Controlled with Low Frequency Alternating Magnetic Field

Irina V. Belyanina[1, 3], Tatiana N. Zamay[1, 3], Galina S. Zamay[1, 2], Sergey S. Zamay[2], Olga S. Kolovskaya[1, 2], Tatiana I. Ivanchenko[1], Valery V. Denisenko[5, 3], Andrey K. Kirichenko[1], Yury E. Glazyrin[1, 2], Irina V. Garanzha[1, 3], Valentina V. Grigorieva[1, 3], Alexandr V. Shabanov[2], Dmitry V. Veprintsev[1, 2], Alexey E. Sokolov[2, 3], Vladimir M. Sadovskii[5, 3], Ana Gargaun[4], Maxim V. Berezovski[4], Anna S. Kichkailo[1, 2]✉

1. Krasnoyarsk State Medical University named after Professor V. F. Voyno-Yasenetsky, Krasnoyarsk, Russia;
2. Federal Research Center, KSC Siberian branch of Russian Academy of Science, Krasnoyarsk, Russia;
3. Siberian Federal University, Krasnoyarsk, Russia;
4. University of Ottawa, Department of Chemistry and Biomolecular Sciences, Ottawa, Ontario Canada;
5. Institute of Computational Modeling RAS SB, Krasnoyarsk, Russia.

✉ Corresponding author: Anna S. Kichkailo, azamay@krasgmu.ru

Received: 2016.08.03; Accepted: 2017.05.29; Published: 2017.07.30

Abstract

Biomedical applications of magnetic nanoparticles under the influence of a magnetic field have been proved useful beyond expectations in cancer therapy. Magnetic nanoparticles are effective heat mediators, drug nanocarriers, and contrast agents; various strategies have been suggested to selectively target tumor cancer cells. Our study presents magnetodynamic nanotherapy using DNA aptamer-functionalized 50 nm gold-coated magnetic nanoparticles exposed to a low frequency alternating magnetic field for selective elimination of tumor cells *in vivo*. The cell specific DNA aptamer AS-14 binds to the fibronectin protein in Ehrlich carcinoma hence helps deliver the gold-coated magnetic nanoparticles to the mouse tumor. Applying an alternating magnetic field of 50 Hz at the tumor site causes the nanoparticles to oscillate and pull the fibronectin proteins and integrins to the surface of the cell membrane. This results in apoptosis followed by necrosis of tumor cells without heating the tumor, adjacent healthy cells and tissues. The aptamer-guided nanoparticles and the low frequency alternating magnetic field demonstrates a unique non-invasive nanoscalpel technology for precise cancer surgery at the single cell level.

Key words: cancer therapy, gold coated magnetic nanoparticles, DNA aptamers, low frequency alternating magnetic field, fibronectin, integrin, apoptosis, necrosis.

Introduction

Medical nanotechnologies are becoming promising for cancer treatment. A variety of nanomaterials and nanoparticles (NPs) have been synthesized for diagnostic and therapeutic applications [1, 2]. At the nanometer scale, materials exhibit novel optical, magnetic, electronic, and structural properties [1, 3], which make nano-sized particles promising tools in molecular diagnostics and anti-cancer therapy [4]. Magnetic nanoparticles (MNPs) can be used as effective heat mediators, drug carriers, and contrast agents [4, 5]. The main drawback is that nanoparticles accumulate in healthy tissues causing harmful effects [6, 7]. Targeted delivery requires functionalization of nanoparticles with molecular probes such as antibodies or aptamers that bind specifically to unique or overexpressed

biomolecules on cancer cells [7, 8]. Aptamers are short synthetic single-stranded DNA or RNA that specifically bind to various targets, such as inorganic ions, small organic molecules, peptides and proteins, whole cells and tissues with high affinity and selectivity [4, 5, 9]. Low immunogenicity, toxicity and cost make aptamers favourable for therapeutic applications [4].

Aptamer-functionalized nanoparticles have been utilized for cancer therapy including photodynamic therapy (PDT) [10] and photothermal therapy (PTT) [11, 12]. PDT is minimally invasive and minimally toxic. It destroys cells by reactive oxygen species generated with light and a photosensitizer. Conjugation of aptamers with nanoparticles improves accumulation of particles in tumor tissue and selective photo-induced damage during PDT. Similar to PDT, PTT is a fairly non-invasive cancer treatment. PTT is based on the ability of gold nanoparticles to absorb light and convert it into heat that promotes destruction of abnormal cells. The effectiveness of this method has been successfully demonstrated on mouse tumor remission [13]. Huang YF *et al.* demonstrated the use of aptamers conjugated to nanorods for targeted PTT of human leukemia [14].

Advantages of PDT and PTT include the less invasive nature of light-based therapies when compared to surgery and the ability to deliver irradiation with great accuracy multiple times over at the same site. However, disadvantages of PDT and PTT include limited accessibility as they can only treat areas that can be reached by light (on or under the skin, or in the lining of organs that can be reached with a light source). Therefore, light-based therapies cannot be used to treat cancers that have grown deeply into the skin or other organs, or cancers that have metastasized.

In this study, we demonstrate the utility of alternative magnetodynamic therapy to eradicate a tumor in mice (Figure 1). We applied aptamer-modified gold-coated magnetic nanoparticles (AGMNPs) to target a tumor *in vitro* and *in vivo*. For the selective targeting, we used aptamer AS-14 to mouse Ehrlich carcinoma fibronectin (Fn) described in our previous study [15]. Fn is a large adhesive glycoprotein that serves as an essential component of the extracellular matrix, which assembles into fibrils, attaching cells to the collagen fibers. It has been shown that besides extracellular Fn, Ehrlich ascites cells synthesize and release large amounts of Fn into the culture medium *in vitro,* and into ascitic fluid and plasma *in vivo* [16]. Fn plays a major role in cell growth, differentiation, migration, wound healing, blood coagulation, embryonic development, and also in oncogenic transformation [17-19]. Fn shows higher expression and different distribution in breast carcinomas than in normal breast parenchyma. Its expression in cancer cell cytoplasm is associated with distant metastasis development and decreased survival rate both in humans and mice [17].

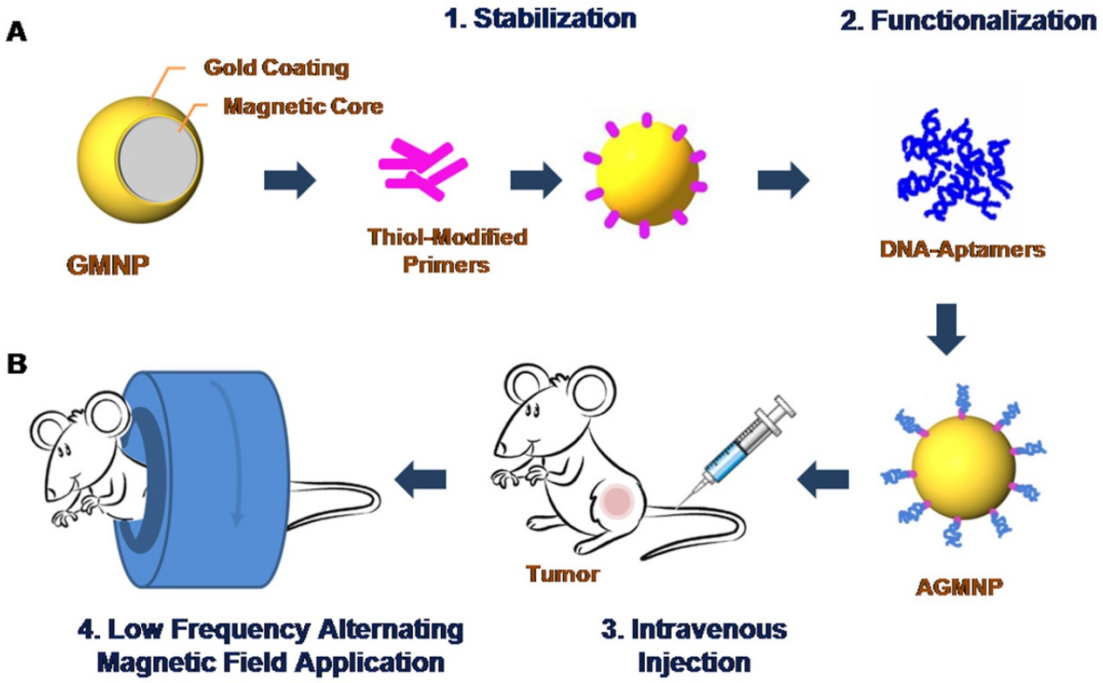

Figure 1. Schematic representation of the modification of gold-coated magnetic nanoparticles (GMNPs) with a thiolated oligonucleotide primer followed by hybridization with a cancer cell specific aptamer (A). Schematic representation of tumor magnetodynamic nanotherapy in a low frequency alternating magnetic field (B).

Aptamer AS-14 delivers GMNPs to Ehrlich carcinoma tumor and links the particles with fibronectin molecules. Fns bind to the cell surface via integrins - large trans membrane adhesion proteins that provide the physical link between the extracellular matrix and the contractile cytoskeleton [20]. Integrins and conventional signalling receptors often cooperate to promote cell growth, cell survival, and cell proliferation [21]. Integrin activation has a structural origin [22, 23], once a ligand binds to it, its head opens the hinge between the β-subunit and hybrid headpiece domain and a mechanical force greatly accelerates the hinge opening [24-26]. Recently reported experimental data and molecular design simulations demonstrate the dynamics of integrin activation due to ligand binding and a mechanical force pulling integrin to 6 nm for 6 ns [24]. Integrin-mediated apoptosis could be induced by its activation followed by direct recruitment and activation of caspase-8 [21, 27-32]. The low frequency alternating magnetic field (LFAMF) causes oscillations of the aptamer-modified GMNPs in complex with fibronectin. Therefore, activity of NPs was modulated by LFAMF. The advantages of the proposed technology include the deep penetration of the magnetic field, high cytotoxic activity toward cancer cells and low toxicity on adjacent cells and healthy tissues.

Materials and Methods

Ethics Statement

This study was carried out in strict accordance with the recommendations in the Guide for the Care and Use of Laboratory Animals of the National Institute of Health. The protocol was approved by the Local Committee on the Ethics of Animal Experiments of the Krasnoyarsk State Medical University. All procedures were performed under anesthesia and all efforts were made to minimize the suffering of animals.

Mouse Tumor Model

White 6-week-old 25 g Imprinting Control Region (ICR) mice were provided by Siberian Federal University. Two million Ehrlich ascites carcinoma cells were transplanted into the right leg of each mouse. On days 5, 7 and 9 after the tumor transplantation, all animals were treated using aptamer AS-14 functionalized gold-coated magnetic nanoparticles in low frequency alternating magnetic field. Ehrlich ascites carcinoma cell cultures were utilized for the *in vitro* studies. Mouse ascites cells were cultured in 35×10 mm cell culture dishes (CELLSTAR®, Germany) in Dulbecco's modified Eagle's medium (DMEM; Sigma-Aldrich), supplemented with 100 UmL^{-1} penicillin, 100 UmL^{-1} streptomycin, and 5% (v/v) fetal bovine serum (FBS) in a humidified atmosphere containing 5% CO_2 at 37°C. All cell experiments were performed in DPBS containing 0.9 mM $CaCl_2$ and 0.49 mM $MgCl_2$.

Low Frequency Magnetic Field Induction

The magnetic coil was specially designed for the magnetodynamic experiments: the copper wire (0.53 mm in diameter) was wound on a cylinder with an inner diameter of 28 mm; the external diameter of the coil was 80 mm, and the resistance of the coil was 21.4 Ω. The coil creates a sinusoidal magnetic field of 100 Oe at a frequency of 50 Hz. The power dissipated in the coil was approximately 1.7 W, which did not heat the coil and sample of cells or the inside of the animal during the procedure. After each treatment, the coil was switched off for 10 minutes in order to avoid the possibility of heating.

Functionalization of Gold-Coated Magnetic Nanoparticles with DNA Aptamers

Gold-coated magnetic nanoparticles (GMNPs) were used with a diameter of 50nm, with a magnetic core of 8-12 nm and a golden shell of 30-40 nm (NITmagoldCit 50nm, Nanoimmunotech, Spain), (Supporting information, Figure S1). Nanoparticles stabilization was carried out with an HPLC purified oligonucleotide complimentary to the 5' of aptamer 5′-CGTGGTTACAGTCAGAGGAGAA-/5ThioMC6-D/-3′ modified at the 3′ position with a 6-hydroxyhexyl disulfide group (Integrated DNA Technologies, USA), in the GMNPs storage buffer for 24 hours at 4°C in a shaker (final concentration of 500nM). This mixture was diluted twice by mixing it with 2×DPBS (with calcium and magnesium) and mixed 1:1 with an equimolar amount of AS-14 aptamer (5′-TCCTCTGACTGTAACCACGAAGGTG TCGGCCTTAGTAAGGCTACAGCCAAGGGAACG TAGCATAGGTAGTCCAGAAGCC-3′), which was previously heated at 95°C for 10 minutes and cooled on ice for 10 minutes, then incubated for an additional 24 hours at 4°C while shaking (Figure 1A).

Optimization of Treatment Conditions for Magnetodynamic Nanotherapy *In Vitro*

One million ascites Ehrlich carcinoma cells in 1 mL of colorless high glucose DMEM medium were incubated with AS-14-GMNPs or non-functionalized GMNPs at 1:25, 1:50, 1:75 or 1:100 ratios (final concentration 1×10^8 particles per 1 mL) or only DPBS with calcium and magnesium for 5, 15 or 30 minutes at 37°C in a humidified atmosphere containing 5% CO_2. All samples were prepared in triplicates. After incubation, the cells were washed twice with the same

buffer and were kept in a magnet producing LFAMF for 1, 3, 5, 7 or 10 minutes. Cell viability was estimated 2 hours after the treatment (cells were captured at 37°C in a humidified atmosphere containing 5% CO_2) using propidium iodide dye (PI) (for timing the treatment procedure). The binding of GMNPs and cell viability were measured using flow cytometry (FC-500, Beckman Coulter, USA).

In Vitro Analyses of the Effects of AMNPs in a Low Frequency Alternating Magnetic Field

Ehrlich carcinoma cells were treated with AS-14-GMNPs or non-functionalized GMNPS at 1:100 ratios (final concentration 1×10^8 particles per 1 mL) or only DPBS for 30 minutes at 37°C in a humidified atmosphere containing 5% CO_2. Then they were washed and kept in a magnet producing LFAMF for 10 minutes. All samples were prepared in triplicates.

Apoptosis induction has been evaluated by caspase cascade activation in tumor cells, after 3 hours of treatment (cells were captured at 37°C in a humidified atmosphere containing 5% CO_2) using CellEvent™ Caspase-3/7 Detection Reagent (5µM in PBS with 5% FBS) (Thermo Fisher Scientific, USA) for 30 minutes at 37°C. The fluorescent signal from CellEvent Caspase-3/7 Detection Reagent was detected using flow cytometry (FC-500, Beckman Coulter, USA). Inhibition of the caspase cascade activation was performed by concurrent binding of antibodies to mouse fibronectin prior to the treatment. The cells were incubated in DPBS / 10% serum to block non-specific protein-protein interactions followed by addition of the primary antibody (anti-fibronectin antibody (TV.1), Abcam, plc., USA,) at a final concentration of 0.7 μgmL^{-1} for 30 min at 37°C. The secondary antibody (donkey anti-rabbit IgG H&L Alexa Fluor® 647, Abcam, plc., USA) was used at 1/2000 dilution for 30 min at 37°C. The control antibody (anti-actin antibody (ACTN05 (C4)), Abcam, plc., USA) was used under the same conditions. Binding was measured using flow cytometry (FC-500, Beckman Coulter, USA).

Apoptosis was evaluated by Annexin V-Cy3 (Sigma Aldrich, USA), phosphatidylserine translocation, and 6-carboxyfluorescein diacetate (6-CFDA) (Sigma Aldrich, USA), which enters the cell and is hydrolyzed by esterases present in living cells to the fluorescent compound 6-carboxyfluorescein, indicating that the cells are viable (for cell death mechanisms identification). The procedures were done in accordance with the manufacturer's protocol and analysed using flow cytometry.

Intracellular sodium content was estimated with a sodium-sensitive dye, SBFI (Thermo Fisher Scientific, USA) by flow cytometry (FC-500, Beckman Coulter, USA) according to the manufacturer's protocols.

In Vivo Antitumor Activity of Aptamer-Modified GMNPs in LFAMF

Six-week-old 25g ICR male mice were used in this study. For two weeks before the experiments, animals were trained to stay calm inside the magnetic coil. Two million Ehrlich's carcinoma cells were transplanted into the right leg of each mouse. Every second day, starting from day five after tumor transplantation until day nine, animals underwent10 minutes of magnetodynamic therapy in LFAMF with aptamer modified magnetic nanoparticles, free nanoparticles, free AS-14 or just DPBS (Figure 1B).

The mice were randomly administered tail vein injections (5, 7 and 9 days after the tumor transplantation, 3 times total) by dividing the mice into four groups with 7 animals in each group as follows:

Group 1: Injection of AS-14-GMNPs in 100 µL DPBS (1.6 $\mu g\ kg^{-1}$);

Group 2: Injection of free GMNPs in 100 µL DPBS (1.6 $\mu g\ kg^{-1}$);

Group 3: Injection of free AS-14 in 100 µL DPBS (0.4 $mg\ kg^{-1}$);

Group 4: Injection of 100 µL DPBS.

After 30 minutes, animals were placed inside the magnet and were treated with a low frequency alternating magnetic field for 10 minutes.

Caspase Activity in Tumor Tissues

To evaluate apoptosis induction by the caspase activity in tumor cells, after 3 hours of treatment a freshly harvested piece of tumor was stained with CellEvent™ Caspase-3/7 (5µM in PBS with 5% FBS) (Thermo Fisher Scientific, USA) for 30 minutes at 37°C, washed with DPBS and fixed with 3.7% formalin. A series of 30µm tissue sections were prepared using cryostat HM 525 (Carl Zeiss, Germany) and fixed on glass slides and imaged with laser scanning microscope (Carl Zeiss LSM780, Germany).

Histological Analysis

To evaluate histological changes of the tumors after magnetodynamic therapy, microscopy of the tissue sections was performed (Axioskop 40, Carl Zeiss, Germany). Tumors were harvested and placed in 3.7% formalin. A series of 10 µm tissue sections were prepared using cryostat HM 525 (Carl Zeiss, Germany) and fixed on glass slides for hematoxylin and eosin staining.

AS-14-GMNPs Distribution in Tumor after Injection in Tail Vein

After injection of AS-14-GMNPs in the tail vein, its distribution in the tumor and other organs was analyzed using electron microscopy on 30μm tissue sections. On the7th day after the tumor transplantation, the mice were injected with GMNPs functionalized with FAM-labeled aptamer AS-14 in 100 μL DPBS (1.6 μg kg^{-1}). After 1, 5 and 24 hours the animals were euthanized and the tumor, liver, kidney and urine were harvested, 30μm tissue sections were prepared using cryostat HM 525 (Carl Zeiss, Germany), fixed on glass slides and placed on silicon foil. Electron microscopy (Hitachi TM3000, Japan) was used to visualize and estimate the percentage ratios of iron and gold. Electron microscopy spectra were processed with the Quantax 70 software (Bruker) for Hitachi TM3000.

Search of Protein Post-Translational Modifications

Search of protein post-translational modifications (PTM) was performed by Proteome Discoverer 1.4 software with Sequest HT search engine. The following seven variable modifications were set: oxidation, deamidation, phosphorylation, glycosylation, acetylation, methylation, acetylation (protein N-terminus). The search results were filtered and only modified peptides were selected. Values of peptide spectra matches (PSM) between modified and non-modified peptides were considered as degrees of modification. Only peptides with prevalence in PSM for modified type or not presented as non-modified were selected as reliable.

In Vivo Toxicity Studies of Aptamer-Modified GMNPs in LFAMF

Healthy 6-week-old 25g ICR mice were used in this study, 10 animals per group. The mice (5 female and 5 male in each group) were administered tail vein injections on days 1, 3 and 5 (3 times total) as follows:

Group 1: Injection of AS-14-GMNPs in 100 μL DPBS (1.6 μg kg^{-1});

Group 2: Injection of 100 μL DPBS.

Toxicity was estimated based on changes in blood biochemistry (cholesterol, total protein, alanine amino-transferase, alkaline phosphatase and bilirubin), which were performed using COBAS INTEGRA 400 plus analyzer (Roche Diagnostics, Switzerland). Male and female parameters were analyzed separately. All data were presented as the mean ± standard error of mean.

Results and Discussion

Our study demonstrates efficacy of targeted GMNPs-based magnetodynamic cancer cell disruption *in vitro* and *in vivo* in a low frequency alternating magnetic field. For the experiments, we used commercially available gold-coated magnetic nanoparticles with a diameter of 50 nm, a magnetic core of 8-12 nm and a 30-40 nm golden shell. The full description is presented in Supporting Information. The magnetic core of the particles provides several magnetodynamic effects on the cells: the golden coating was used to attach aptamers to the surface through SH groups, furthermore, coating the iron particles with gold reduces their toxicity and increases their biocompatibility *in vivo*. The behaviour of aptamer-modified GMNPs in a magnetic field of alternating frequency in a colloid solution in DPBS at a concentration of 1×10^8 particles per 1 mL, which was suitable for the therapeutic purposes, was estimated using magnetic circular dichroism (MCD). At a frequency of 50 Hz, the MCD of the particles *in vitro* in a sinusoidal magnetic field sufficiently increased and all particles magnetized (Figure S1).

Mathematical simulations showed that a sinusoidal magnetic field of 100 Oe at a frequency of 50 Hz induced magnetodynamic cell disruption with minimal possible thermal effects on cells and tissues (Supporting Information) therefore it could be used for magnetodynamic purposes. For selective targeting we used aptamer AS-14 to mouse Ehrlich carcinoma fibronectin (Fn) described in our previous study [15]. Here we revealed that Fn from Ehrlich carcinoma cells recognized by aptamer AS-14 has several post-translational modifications in the 5 domains of Fn type III ($FnIII_5$): threonine is acetylated at position 32 and phosphorylated at position 36. These modifications are not currently described in the Protein Data Bank http://www.rcsb.org/pdb/protein/P02751, therefore, suggest they are unique to mouse Ehrlich carcinoma cells. Potentially, aptamer AS-14 recognizes particularly this region, which is located between collagen binding and cell attachment sites.

Aptamer AS-14 delivers the GMNPs to the Ehrlich carcinoma tumor and links the particles with fibronectin molecules. The low frequency alternating magnetic field forces the GMNPs in complex with the aptamers bound to fibronectin to oscillate. The mathematical modeling of the magneto-mechanical action of AS-14-GMNPs on cells is described in Supporting Information. Interestingly, LFAMF did not cause local hyperthermia (Supporting Information). LFAMF rotates a nanoparticle bound to $FnIII_5$ clockwise pulling the integrin β-subunit via $FnIII_{10}$ and returns it to its original position (Figure 2).

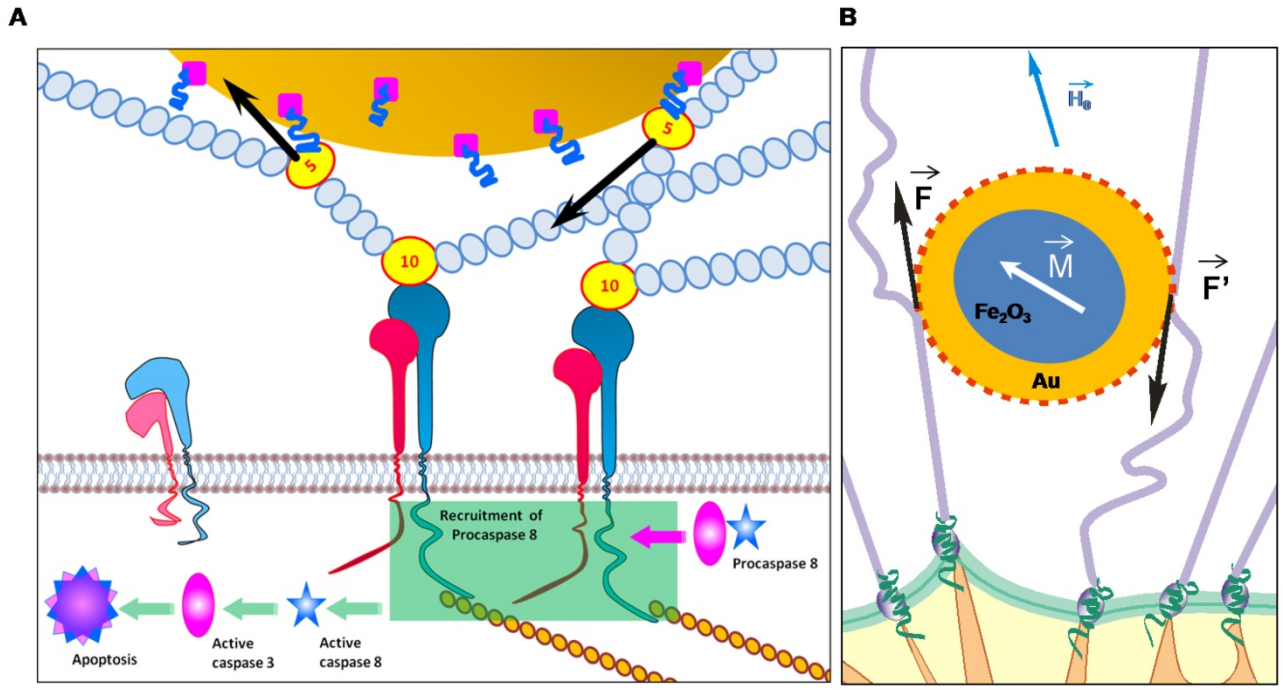

Figure 2. Schematic representation of an apoptotic caspase cascade. (A) The cascade is caused by fibronectin oscillations in a low frequency alternating magnetic field controlled by AS-14-GMNPs. (B) Forces applied to an AS-14-GMNP in the presence of a low frequency alternating magnetic field, where $\vec{F}$ – is the force pulling fibronectin; $\vec{M}$ – is the magnetic moment of GMNP; and $\vec{H}_0$ –is an external magnetic field.

We calculated the magnetic moment, force and time of action of the magnetic particles in LFAMF (Supporting Information). LFAMF with a frequency of 50 Hz makes AS-14-GMPS periodically pull and relax the C terminus of $FnIII_{10}$ to 0.07 nm for 0.01 seconds, that means twice per period of LFAMF variation. Mechanical forcepulling of integrin activates FnIII [24] and causes integrin-mediated apoptosis by direct recruitment and activation of caspase-8 [21, 27-32]. We think that the oscillations of AS-14-GMNPscaused by LFAMF influences integrins via Fn and causes activation of caspases followed by cell apoptosis (Figure 2).

Effects of Aptamer-Modified GMNPs in LFAMF *In Vitro*

In order to optimize the therapeutic procedure *in vitro*, titration experiments at different incubation times have been performed. Incubation time did not influence binding much, as after 5 minutes, most cells appeared to be bound with aptamer-modified fluorescently-labeled nanoparticles, with 75 and 100 particles bound per cell. Binding of 25 and 50 particles per cell required more time for efficient binding (Figure 3A).

One hundred particles per cell was enough to prompt binding, therefore this concentration was chosen for *in vitro* experiments and to insure all cells specifically bound to the particles, incubation time was always 30 minutes. To adjust the time of LFAMF exposure, Ehrlich carcinoma cells bound with AS-14-GMNPs (a ratio of 1:100 particles after 30 minutes of incubation) were placed in the center of the magnetic coil in LFAMF for 1, 3, 5, 7, and 10 minutes (Figure 3). The cellular death was registered two hours after the treatment using propidium iodide (PI) dye by flow cytometry. Ten minutes were sufficient to induce death of Ehrlich carcinoma cells and to avoid heating of the magnetic coil during this time.

In order to prove our proposal that the oscillations of AS-14-GMNPs bound with Fn in LFAMF pull integrins via Fn and result in activation of caspases cascade (Figure 2), we performed binding experiments with anti-Fn antibodies that block the interaction of AS-14 with Fn (Figure 4). Three hours after treatment with AS-14-GMNPs in LFAMF activation of caspase 3/7 occurred in 35% of cells. The anti-Fn antibodies added to the cells prior to the treatment occupied the binding sites for AS-14-GMNPs and inhibited caspase cascade, while the control anti-actin antibody did not (Figure 4A1).

In intact cells caspase 3/7 was activated in 11% of cells, treatment with GMNPs in LFAMF increased fluorescence intensity, but not the number of apoptotic cells (Figure 4A2). We should note that these experiments were performed in cell cultures which grew in suspension and thus express less extracellular Fn, than in solid tumor *in vivo* [16]. Anti-Fn antibodies bond to only 60% of cells (Figure 4B).

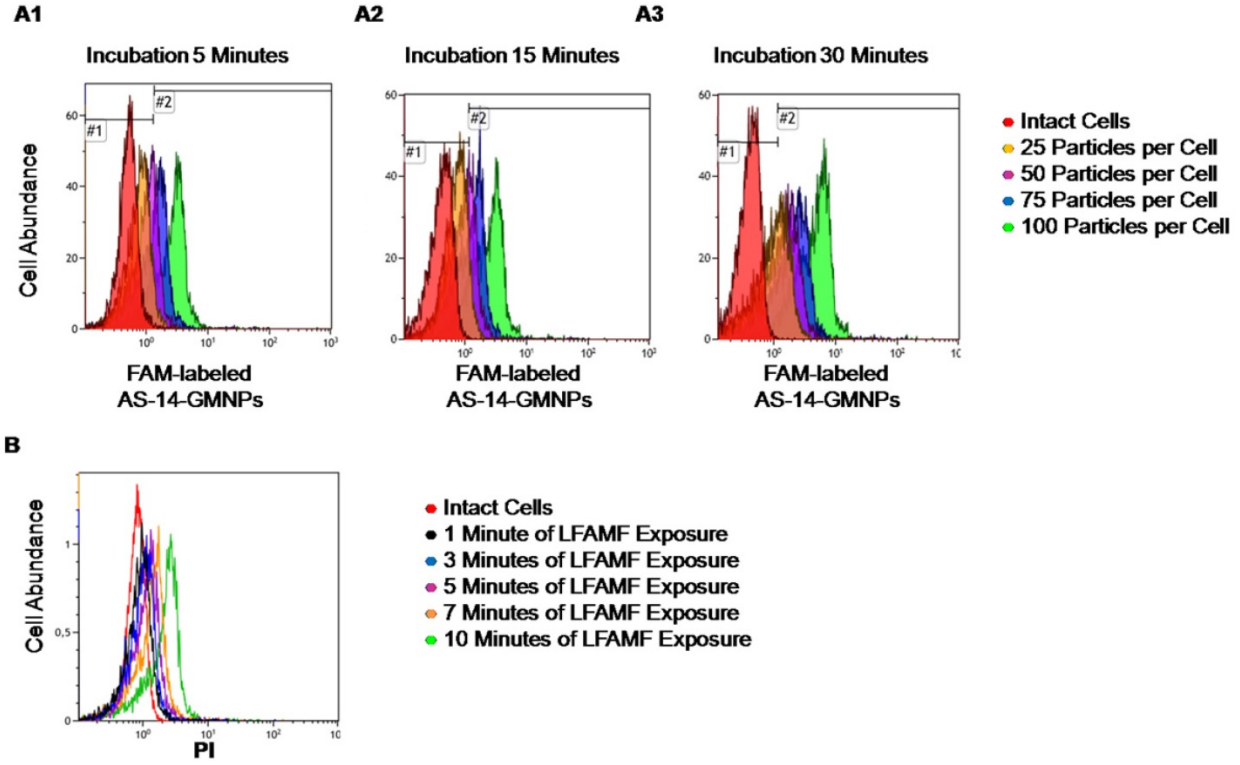

Figure 3. Optimization of treatment conditions for magnetodynamic nanotherapy *in vitro*. (A) Determination of the binding time for different amounts of AS-14 modified GMNPs per cell. Histograms for binding of 25 particles per cell (orange); 50 particles per cell (purple); 75 particles per cell (blue), and 100 particles per cell (green) after 5 minutes (A1); 15 minutes (A2), and 30 minutes of incubation (A3). (B) Viability of Ehrlich cells pre-incubated with AS-14-GMNPs (ratio of 100 particles per cell for 30 minutes) after 1, 3, 5, 7, and 10 minutes of LFAMF exposure.

In cell culture experiments, we demonstrated that AS-14-GMNPs in LFAMF induced carcinoma cell death, which was started with apoptotic phosphatidylserine translocation and was followed by necrosis (Figure 4 C5). After the AS-14-GMNPs - LFAMF treatment, the majority of Annexin V positive cells were also CFDA negative (which indicates they were dead). Control experiments with AS-14-GMNPs alone without a magnetic field and GMNPs without aptamers with LFAMF treatment did not cause carcinoma cells death, but the cells accumulated less CFDA, and their membranes might have been slightly damaged. Moreover, the content of sodium cations in carcinoma cells increased after treatment with AS-14-GMNPs in LFAMF, suggesting necrosis (Figure 4D). Cell death can be caused by activation of different molecular pathways, including apoptosis, necrosis and autophagy, characterized by morphological and biochemical features [33]. Death processes are accompanied by a change in the cell volume due to a change in ion fluxes, especially sodium ions. Significant loss of sodium, potassium and chlorine ions are essential for activation of caspases and nucleases for apoptosis development [34]. In contrast, necrosis, is characterized by swelling of the cell because of increased sodium content. The lack of energy for Na^+/ K^+-ATPases in cellular necrosis causes swelling of cell followed by membrane rupture and inflammation.

In Vivo Antitumor Activity of Aptamer-Modified GMNPs in LFAMF

In vivo antitumor efficacy of AS-14-GMNPs in LFAMF was evaluated using solid Ehrlich carcinoma in which the tumor was transplanted into the right leg of each mouse. The principal scheme of the experiment is presented in Figure 1 and described in details in the Materials and Methods sections. Briefly, AS-14 modified GMNPs (1.6 μg kg^{-1}), free GMNPs, free AS-14 (0.4 mg kg^{-1}) and DPBS for control groups (7 animals in each) were injected intravenously, and after 30 minutes, LFAMF was applied for 10 minutes. The treatment procedures were repeated three times on alternate days starting on day 5 after tumor transplantation.

The efficacy of the treatment is presented in Figure 5A: tumor sizes were estimated by measuring the leg girth regularly every day after treatment. The tumor size visually decreased after treatment with AS-14-GMNPs and LFAMF. On day 6, after the first treatment, a subcutaneous hemorrhage was observed in the leg with the tumor in each mouse injected with AS-14-GMNPs and exposed with LFAMF for 10 min (Figure 5B). On day 8, after a second treatment was

performed on day 7, the tumor stopped growing and formed a crust, suggesting necrosis. After the third injection, on day 9, the wound began to heal. On day 13, the size of the crust reduced significantly and the skin around it almost fully recovered. Treatment with either GMNPs or AS-14 aptamer in LFAMF did not cause any reduction in tumor size. Injection of GMNPs with LFAMF exposure caused a slight inflammation in the tumor, which grew during the course of treatment, demonstrating the minor effect of GMNPs. We believe that GMNPs themselves also cause tumor necrosis, but they are sufficiently less effective without the aptamer.

Mathematical simulations show that LFAMF alone does not cause hyperthermia or in the presence of GMNPs and AS-14-GMNPs. Therefore, the mechanical action of LFAMF on GMNPs linked through the aptamer with tumor cells can be explained as follows: Fn causes twitching of the integrin β-domain which leads to its activation [24] and initiation of cell death by the caspase cascade induction of primary apoptosis (Figure 2A) followed by an increase in sodium content (Figure 4B) and cancer cell necrosis (Figure 6 B10-B12). Considerable damage of the tumor *in vivo* and tumor size reduction by LFAMF occurred only when the GMNPs were aptamer modified and delivered to the tumor site (Figure 5). For non-specific accumulation of GMNPs in tumor, the effect was insufficient and may be a result of the 30-minute exposure time.

Aptamer-facilitated magnetodynamic nanotherapy at a low frequency (50 Hz) of alternating magnetic field did not cause local hyperthermia, which was demonstrated by mathematical simulations (Supporting Information).

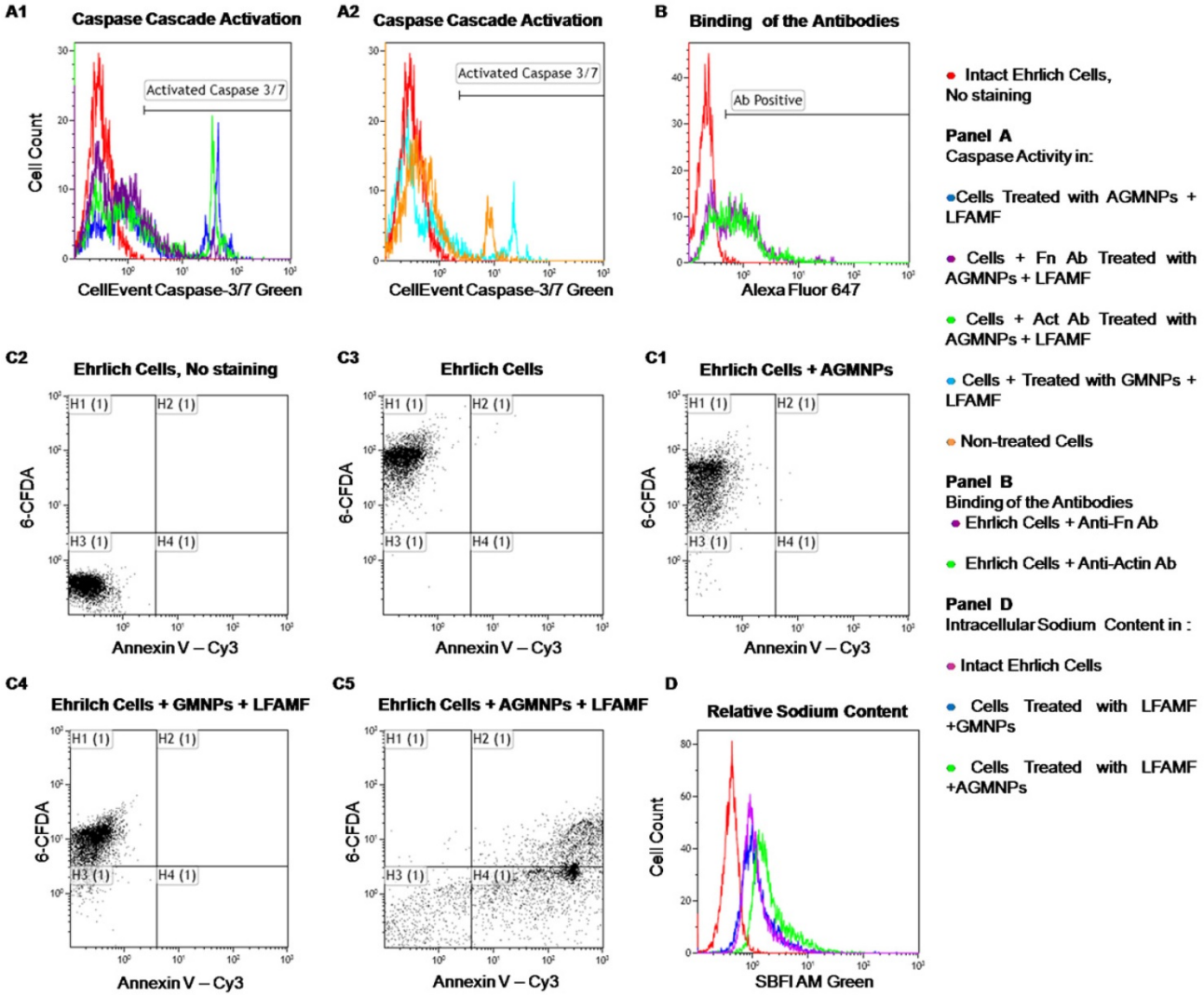

Figure 4. Mechanisms and efficacy of magnetodynamic nanotherapy *in vitro*. (**A**) Apoptosis estimated by caspase 3/7 activity; (**B**) Apoptosis estimated by Annexin V-Cy3 labeling and 6-carboxyfluorescein diacetate (6-CFDA) staining of Ehrlich cells: (1) intact cells without staining; (2) viability of living cells; (3) cells 3 hours after exposure to LFAMF; (4) cells 3 hours after treatment with GMNPs and LFAMF; (5) cells 3 hours after treatment with AS-14-GMNPs (AGMNPs) and LFAMF. (B) Relative sodium content estimated by SBFI fluorescence intensity: the red curve corresponds to cells without staining, the purple - to untreated cells; the blue - to cells treated with GMNPs in LFAMF; and green to cells treated with AS-14-GMNPs in LFAMF.

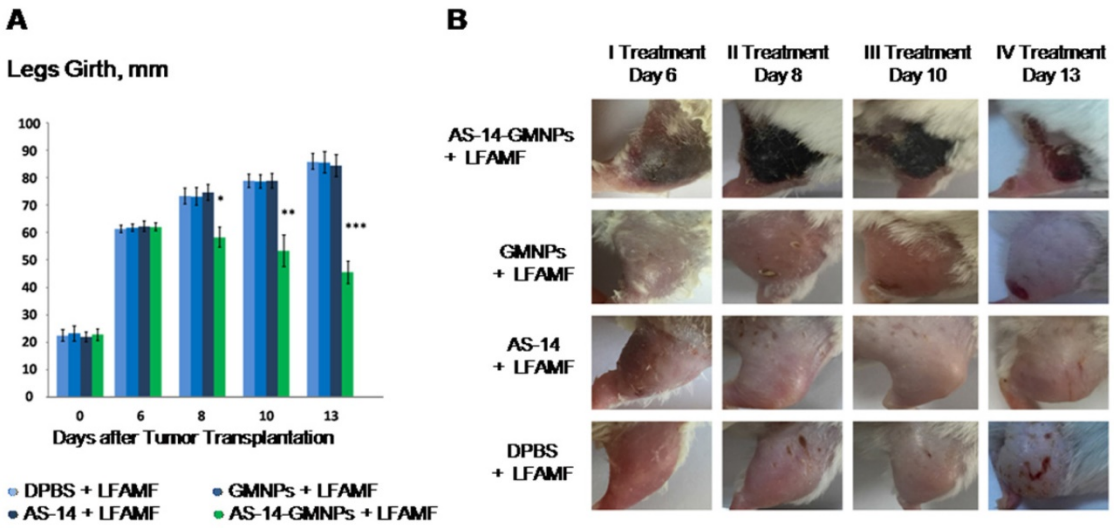

Figure 5. Efficacy of magnetodynamic nanotherapy *in vivo*. (A) Tumor size changes during the course of treatment (* p<0.05; ** p<0.01; *** p<0.001). (B) Imaging of the tumor recovery after LFAMF treatment.

Tissue Analyses after Magnetodynamic Nanotherapy

We identified that a reduction in tumor size was due to the mechanical oscillations of AS-14-GMNPS in LFAMF. Five hours after the treatment with AS-14-GMNPs in LFAMF, caspase 3/7 were active in tumor cells (Figure 6A), whereas pure GMNPs or free AS-14 aptamer in LFAMF did not cause this effect.

Tumors did not respond to the control treatment with pure DPBS in LFAMF; cells stayed viable, tumors grew and destroyed muscle tissue, and the immune response was weak (Figure 6 B1-3). The control treatment with free aptamer AS-14 in DPBS and LFAMF did not show significant changes in the tumor's structure; lymphocytic infiltration was still poor, swelling of the intermediate spaces was moderate, and muscle fibers were degenerative (Figure 6, B4-6).

Treatment with pure GMNPs caused partial necrosis of tumor tissues remaining in the form of "islands" (Figure 6, B7-B9). We observed tumor cells with cytoplasm vacuolization and signs of karyolysis, which is an irreversible result of the damaging effects of the treatment (Figure 6, B9). Inflammatory lymphocytic infiltration was expressed weakly around the tumor (Figure 6, B7-B9).

A significant therapeutic effect was observed in tumor tissues after treatment with AS-14-GMNPs in LFAMF (Figure 6 B9-B12). On the periphery of the large tumor necrosis areas remained small amounts of carcinoma cells, partly subjected to complete destruction or with irreversible changes: karyorrhexis, karyolysis, plasmorrhexis, these were the damaging effects of the treatment (Figure 6 B12). This treatment caused significant immune response as there was visible inflammatory infiltration of segmented leukocytes on the boundaries of necrotic areas. Swelling and destructive changes of the tumor tissue's microenvironment were also observed (Figure 6 B9-B12).

Toxicity of aptamer-functionalized GMNPs was estimated by changes in blood serum biochemistry (Table 1). In addition, we attempted to estimate iron and gold distribution in different organs after intravenous injection of AS-14-GMNPs in DPBS (Figure S2). Electron microscopy revealed that a single dose of AS-14-GMNPs (1.6 μg kg^{-1}) is not sufficient for detection of iron and gold ions in the tumor, other organs and urine after 1, 5 and 24 hours (Figure S2). Cholesterol, serum alanine amino-transferase (ALT), alkaline phosphatase (ALP) and bilirubin are the standard parameters for drug hepatotoxicity evaluation [35]. ALT is involved in energy metabolism in the liver, with lower enzymatic activities in other tissues, therefore it is considered as a specific biomarker of liver function. Total bilirubin, a product of hemoglobin degradation, is a marker of hepatobiliary injury and hemolysis [35]. ALP is associated with cell membrane damage of hepatocytes [35]. In our experiments, 3 injections of AS-14-GMNPs administered to healthy male and female mice did not cause changes in these parameters compared to the control group treated with DPBS and was not dependent on gender. Inflammation and hydration status of the animals treated with nanoparticles was evaluated by total protein concentration [35], which did not significantly differ in the groups of male and female mice treated with AS-14-GMNPs (Table 1). All tested parameters indicate that the treatment with AS-14-GMNPs is safe and does not cause hepatotoxic effects.

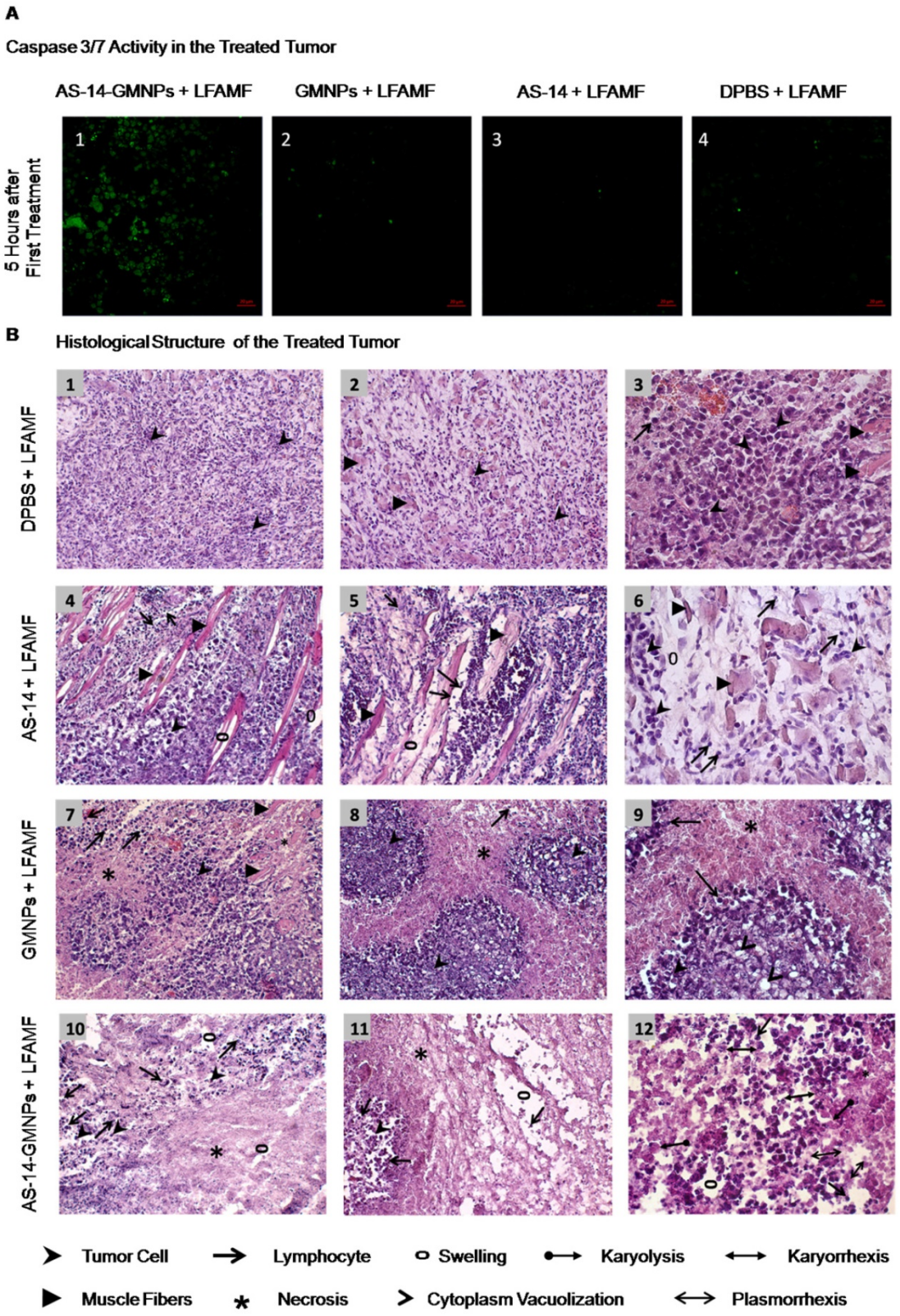

Figure 6. Tumor response to magnetodynamic nanotherapy. (**A**) Caspase 3/7 activity in cancer cells from tissue sections of tumors harvested 5 hours after treatment. (**B**) Histological structure of treated tumors. **B1-B3** – DPBS and LFAMF treated Ehrlich carcinoma has a solid structure and grows into the muscle tissue, composed of atypical cells with pleomorphic, hyperchromatic nuclei of different shapes and volume. No immune response: very rare lymphocytes. **B4-B6** – AS-14 and LFAMF treated carcinoma has moderate swelling of the intermediate spaces, poor lymphocytic infiltration and muscle fibers with degenerative changes. **B7-B9** – GMNPs and LFAMF treated carcinoma displays scattered tumor necrosis with weakly expressed inflammatory infiltration, tumor tissue remains in the form of "islands" in which the majority of cancer cells are with cytoplasm vacuolization and signs of karyolysis. **B10-B12** – AS-14-GMNPs and LFAMF treated carcinoma shows large tumor necrosis areas, swelling, destructive changes of tumor tissue microenvironment and inflammatory infiltration of segmented leukocytes. On the periphery remaining tumor cells are dead with karyorrhexis, karyolysis, plasmorrhexis. Magnification: (B1) ×100; (B2, B4, B5, B7, B8, B10, B11) × 200; (B3, B6, B9, B12) ×400.

Table 1. Blood serum biochemistry parameters performed separately for male and female mice treated with AS-14-GMNPs in phosphate buffer (DPBS) or DPBS alone. All data are presented as the mean ± standard error of mean.

Sample	Cholesterol, m mole L^{-1}	Total protein, g L^{-1}	Alanine amino-transferase, IU L^{-1}	Alkaline phosphatase, IU L^{-1}	Total bilirubin, μ mole L^{-1}
AS-14-GMNPs					
Female (N=5)	1.45±0.01	50.75±3.32	18.40±3.67	214.30±74.81	5.67±0.38
Male (N=5)	1.56±0.48	55.97±6.21	31.90±13.17	254.87±122.29	6.05±0.21
DPBS					
Female (N=5)	2.30±0.28	53.90±1.27	13.55±4.78	177.67±27.13	6.25±0.70
Male (N=5)	2.32±0.26	55.90±2.76	20.93±6.9	251.40±71.13	6.20±0.53

Conclusion

Our study demonstrates the therapeutic effect of magnetodynamic nanotherapy guided by cell specific aptamers on cancer. Further investigations need to be performed to better understand the mechanism of action of AS-14-GMNPs in LFAMF and overall toxicity of AS-14-GMNPs and LFAMF on normal tissues. Promising opportunities for effective applications of the proposed method are based on using aptamer-functionalized gold- coated magnetic nanoparticles for targeted tumor treatment in a low frequency alternating magnetic field, which selectively destroys cancer cells without affecting non-malignant adjacent cells and tissues.

Acknowledgements

The authors are grateful to George Y. Vorogeikin, Yuri I. Vorogeikin and "OKB ART". Andrey Barinov and "OPTEC Group"for help with 3D laser scanning imaging. Microscopic analyses using Carl Zeiss LSM 800 were done in the "Center for bioassay, nanotechnology and nanomaterials safety" ("Biotest-Nano") (Multiple-Access Center, Tomsk State University, Tomsk, Russia). Toxicity studies have been performed in Multiple-Access Center, Central Scientific Research Laboratory in Krasnoyarsk State Medical University named after prof. V.F. Voino-Yasenecky. This work was supported by the Russian Scientific Fund (grant #14-15-00805).

Supplementary Material

Supporting information.
http://www.thno.org/v07p3326s1.pdf

Competing Interests

The authors have declared that no competing interest exists.

References

1. El-Sayed M. Small is different: Shape-, size-, and composition-dependent properties of some colloidal semiconductor nanocrystals. Acc Chem Res. 2004; 37: 326-33.
2. Huang X, Jain P, El-Sayed I, El-Sayed M. Gold nanoparticles: interesting optical properties and recent applications in cancer diagnostic and therapy. Nanomedicine. 2007; 2: 681-93.
3. Davis M, Chen Z, Shin D. Nanoparticle therapeutics: an emerging treatment modality for cancer. Nat Rev Drug Discov. 2008; 7: 771-82.
4. Liu Q, Jin C, Wang Y, Fang X, Zhang X, Chen Z, et al. Aptamer-conjugated nanomaterials for specific cancer cell recognition and targeted cancer therapy. NPG Asia Mater. 2014; 6.
5. Malik M, O'Toole M, Casson L, Thomas S, Bardi G, Reyes-Reyes E, et al. AS1411-conjugated gold nanospheres and their potential for breast cancer therapy. Oncotarget. 2015; 6: 22270-81.
6. Banerjee R, Katsenovich Y, Lagos L, McIintosh M, Zhang X, Li C. Nanomedicine: Magnetic Nanoparticles and their Biomedical Applications. Curr Med Chem. 2010; 17: 3120-41.
7. Dreaden E, Alkilany A, Huang X, Murphy C, El-Sayed M. The golden age: gold nanoparticles for biomedicine. Chem Soc Rev. 2012; 41: 2740-79.
8. Wu P, Gao Y, Lu Y, Zhang H, Cai C. High specific detection and near-infrared photothermal therapy of lung cancer cells with high SERS active aptamer-silver-gold shell-core nanostructures. Analyst. 2013; 138: 6501-10.
9. Gu F, Karnik R, Wang A, Alexis F, Levy-Nissenbaum E, Hong S, et al. Targeted nanoparticles for cancer therapy. Nano Today. 2007; 2: 14-21.
10. Bugaj AM. Targeted photodynamic therapy - a promising strategy of tumor treatment. Photoch Photobio Sci. 2011; 10: 1097-109.
11. Luo YL, Shiao YS, Huang YF. Release of Photoactivatable Drugs from Plasmonic Nanoparticles for Targeted Cancer Therapy. ACS Nano. 2011; 5: 7796-804.
12. Hu XG, Gao XH. Multilayer coating of gold nanorods for combined stability and biocompatibility. Phys Chem Chem Phys. 2011; 13: 10028-35.
13. Shi H, Ye XS, He XX, Wang KM, Cui WS, He DG, et al. Au@Ag/Au nanoparticles assembled with activatable aptamer probes as smart "nano-doctors" for image-guided cancer thermotherapy. Nanoscale. 2014; 6: 8754-61.
14. Huang YF, Sefah K, Bamrungsap S, Chang HT, Tan W. Selective Photothermal Therapy for Mixed Cancer Cells Using Aptamer-Conjugated Nanorods. Langmuir. 2008; 24: 11860-5.
15. Kolovskaya OS, Zamay TN, Zamay AS, Glazyrin YE, Spivak EA, Zubkova OA, et al. DNA-Aptamer/Protein Interaction as a Reason of Apoptosis and Proliferation Stop in Ehrlich Ascites Carcinoma Cells. Biol Membr. 2013; 30: 398-411.
16. Zardi L, Cecconi C, Barbieri O, Carnemolla B, Picca M, Santi L. Concentration of fibronectin in plasma of tumor-bearing mice and synthesis by Ehrlich ascites tumor cells. Cancer Res. 1979; 39: 3774-9.
17. Fernandez-Garcia B, Eiro N, Marin L, Gonzalez-Reyes S, Gonzalez L, Lamelas M, et al. Expression and prognostic significance of fibronectin and matrix metalloproteases in breast cancer metastasis. Histopathology. 2014; 64: 512-22.
18. Pankov R, Yamada K. Fibronectin at a glance. J Cell Sci. 2002; 115: 3861-3.
19. Ritzenthaler J, Han S, Roman J. Stimulation of lung carcinoma cell growth by fibronectin-integrin signalling. Mol Biosyst. 2008; 4: 1160-9.
20. Hynes R. The emergence of integrins: a personal and historical perspective. Matrix Biol. 2004; 23: 333-40.
21. Campbell I, Humphries M. Integrin Structure, Activation, and Interactions. Cold Spring Harb Perspect Biol. 2011; 3.
22. Luo B, Carman C, Takagi J, Springer T. Disrupting integrin transmembrane domain heterodimerization increases ligand binding affinity, not valency or clustering. Proc Natl Acad Sci USA. 2005; 102: 3679-84.
23. Takagi J, Springer T. Integrin activation and structural rearrangement. Immunol Rev. 2002; 186: 141-63.
24. Puklin-Faucher E, Gao M, Schulten K, Vogel V. How the headpiece hinge angle is opened: new insights into the dynamics of integrin activation. J Cell Biol. 2006; 175: 349-60.
25. Puklin-Faucher E, Sheetz M. The mechanical integrin cycle. J Cell Sci. 2009; 122: 179-86.
26. Puklin-Faucher E, Vogel V. Integrin Activation Dynamics between the RGD-binding Site and the Headpiece Hinge. J Biol Chem. 2009; 284: 36557-68.
27. Danen E. Integrin Proteomes Reveal a New Guide for Cell Motility. Sci Signal. 2009; 2.
28. Danen E, Ruiter D, Vanmuijen G. Mechanisms of Melanoma Cell-Adhesion to Fibronectin. Biochem Soc Trans. 1995; 23: S403-S.
29. Danen E, Sonnenberg A. Integrins in regulation of tissue development and function (vol 200, pg 471, 2003). J Pathol. 2003; 201: 632-41.
30. Danen E, Sonneveld P, Sonnenberg A, Yamada K. Dual stimulation of Ras/Mitogen-activated protein kinase and RhoA by cell adhesion to fibronectin supports growth factor-stimulated cell cycle progression. J Cell Biol. 2000; 151: 1413-22.

31. Danen E, van Rheenen J, Franken W, Huveneers S, Sonneveld P, Jalink K, et al. Integrins control motile strategy through a Rho-cofilin pathway. J Cell Biol. 2005; 169: 515-26.
32. Zhang Y, Chen M, Venugopal S, Zhou Y, Xiang W, Li Y, et al. Isthmin exerts pro-survival and death-promoting effect on endothelial cells through alphavbeta5 integrin depending on its physical state. Cell Death Dis 2011; 2.
33. Bortner C, Cidlowski J. Ion channels and apoptosis in cancer. Philos Trans R Soc Lond B Biol Sci. 2014; 369.
34. Bortner C, Cidlowski J. Uncoupling cell shrinkage from apoptosis reveals that Na+ influx is required for volume loss during programmed cell death. J Biol Chem. 2003; 278: 39176-84.
35. A. Wallace Hayes, Claire L. Kruger. Hayes' Principles and Methods of Toxicology, Sixth Edition. 2014; 824.